

INSTITUTO DE COMPUTAÇÃO
UNIVERSIDADE ESTADUAL DE CAMPINAS

**Reconnection of fingerprint ridges
based on morphological operators and
multiscale directional information**

M. A. Oliveira *N. J. Leite*

Technical Report - IC-04-05 - Relatório Técnico

June - 2004 - Junho

The contents of this report are the sole responsibility of the authors.
O conteúdo do presente relatório é de única responsabilidade dos autores.

Reconnection of fingerprint ridges based on morphological operators and multiscale directional information

Marcelo de Almeida Oliveira* Neucimar Jerônimo Leite*

June 7th, 2004

Abstract

In this paper, we introduce a multiscale operator which, together with some morphological tools, can be used to reconnect broken components of an image. This operator extracts the orientation field from the image components and can be applied to both binary and gray-scale pictures. Although we illustrate its application in the fingerprint domain, the approach described here can be easily extended to images whose components exhibit well-defined directional information.

Key-words: Fingerprints, Multiscale Directional Information, Mathematical Morphology, Watersheds.

1 Introduction

Nowadays, there is an increasing emphasis on the privacy and security of personal information and, therefore, the importance of accurate personal identification systems has also increased.

In order to satisfy this requirement, automatic fingerprint identification systems (AFISs) were created and became the most widely used biometric technology [1] due to the following fingerprint characteristics:

- *Universality*: everyone has it;
- *Permanence*: remains invariant over lifetime;
- *Collectability*: easy to be collected;
- *Distinctiveness*: it is sufficiently different from one person to another, even in cases of identical twins [2].

Most automatic fingerprint identification systems are based in minutiae matching [3, 4, 5, 6]. *Minutiae* are local discontinuities in the fingerprint pattern. The most important ones are *ridge ending* and *ridge bifurcation*, illustrated in figure 1.

*Institute of Computing, University of Campinas, 13084-971, Campinas, SP. Research supported by FAPESP — Fundação de Amparo à Pesquisa do Estado de São Paulo, grant by process number 03/01907-8

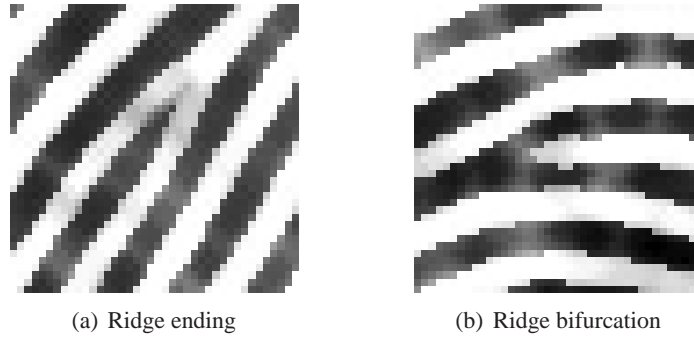


Figure 1: Examples of minutiae.

The main difficulty for minutiae extraction is that fingerprint quality is often too low, thus noise and contrast deficiency can produce false minutiae or hide valid ones. Even high quality images can yield false minutiae, for example, when the person has cuts or scars in her fingers.

To solve these problems, several approaches have been developed for fingerprint image enhancement, using Fourier transform [7, 8], Wavelet transform [9], Gabor filters [5, 10, 11] etc, and for minutiae filtering, applied to binary [12, 13, 14, 15] or gray-scale images [16].

This work considers the problem of reconnecting broken ridges in fingerprint images based on morphological operators and multiscale directional information, obtained by the neighborhood operator introduced here, which yield more accurate results than the typical approaches using image gradient operator [3, 5, 11]. This reconnection method can be used to improve ridge following algorithms [4, 17] and minutiae extraction steps. It also turns the minutiae filtering step unnecessary.

Although we focus this paper on the fingerprint domain, the method described is quite general and can be easily extended to connect image components whose features can be associated with directional information. This is the case of applications concerning areas such as medicine, biometrics, metallurgy and geology.

2 Mathematical Morphology

Our approach for reconnecting fingerprint ridges is based mainly on some mathematical morphology transformations [18, 19, 20], briefly discussed in this section, and on the gray-scale directional operator introduced in section 3.1.

2.1 Erosion and Dilation

Erosion and dilation constitute the basis for more complex morphological operators and can be defined as follows.

Let $f : Z^2 \rightarrow Z$ be a gray-scale image and $b : Z^2 \rightarrow Z$ a plain structuring element. The gray-scale erosion of f by b , denoted by $f \ominus b$, is defined as

$$(f \ominus b)(x, y) = \min\{f(x + s, y + t) - b(s, t)\}, \quad (1)$$

where $(x + s, y + t) \in \mathcal{D}_f$, $(s, t) \in \mathcal{D}_b$ and \mathcal{D} represents the discrete domain of the images.

The gray-scale dilation of f by b , denoted by $f \oplus b$, is defined as

$$(f \oplus b)(x, y) = \max\{f(x - s, y - t) + b(s, t)\}, \quad (2)$$

where $(x - s, y - t) \in \mathcal{D}_f$ and $(s, t) \in \mathcal{D}_b$.

2.2 Closing and Opening

By iteratively applying erosion and dilation, one can eliminate image details, smaller than the structuring element, without affecting its global geometric features.

Visually, closing smoothes the contours, fills narrow gulfs and eliminates small holes. The gray-scale closing of f by b , denoted by $f \bullet b$, is defined as

$$(f \bullet b) = (f \oplus b) \ominus b \quad (3)$$

On the other hand, opening smoothes contours, break narrow isthmuses and eliminates small islands. The gray-scale opening of f by b , denoted by $f \circ b$, is defined as

$$(f \circ b) = (f \ominus b) \oplus b \quad (4)$$

2.3 Watersheds

The watershed is a very important morphological tool used in image segmentation and an intuitive definition of this transformation is given here. Formal definitions can be found, for instance, in [20, 21].

Let f be a gray-scale image and $m_i(f)$ its regional minima. Now, consider f as a topographic surface where the gray value of each pixel represents the altitude and each minimum $m_i(f)$ is pierced. We will flood this topographic surface by submerging it into a lake with a constant vertical speed. During the flooding process, two or more floods coming from different minima may merge. Every time it happens, we build a dam at the points where the floods would merge. At the end of the process, only the dams emerge. These dams define the watershed lines of the image f , segmenting the image in several basins $b_i(f)$. Each basin $b_i(f)$ contains one and only one minimum $m_i(f)$ and corresponds to the influence zone of this minimum.

3 Reconnecting fingerprint ridges

In this section, we introduce an approach for reconnecting fingerprint ridges. Figure 2 shows a general flowchart of the method which consists mainly of the following steps:

- *Orientation field estimation*: this step computes the most likely orientation of each pixel in the fingerprint image.
- *Image enhancement by watersheds*: the watershed transform gives the influence zone of all regional minima of the image. Note that in the binary case, it defines the influence zone of each ridge.

- *Definition of markers*: a subset of the watershed lines, representing regions of broken ridges, is obtained at this step.
- *Estimation of the distance between broken ridges*: the distance transform is applied to a set defined from the difference between two orientation field scales which results in an estimate of the distance between broken ridges.
- *Directional opening by markers*: to reconnect the broken components, a directional morphological opening is executed in the regions defined by the markers, where the opening size parameter is estimated from the distance between broken ridges.

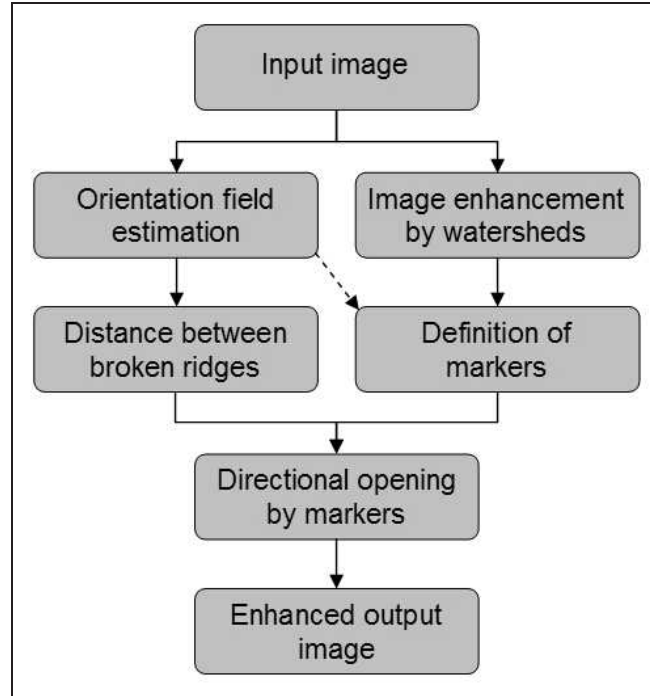


Figure 2: General flowchart of the proposed method.

Next, we describe with some details each of these steps.

3.1 Orientation field estimation

In this section, we focus our discussion on the orientation field estimation of a gray-scale fingerprint image, although the method introduced here can be applied to any kind of image (even binary, as we will see in section 3.3) whose components exhibit well-defined directional information.

The following definitions are necessary for the method description. Let D be the number of directions to be considered in a given neighborhood and n the number of pixels considered in each of these directions. From now on, we refer to these pixels as *test points*. Note that to represent all D directions in a two-dimensional grid, the number n of test points has a minimum bound, that is, for n test points, we can define up to $(2 \cdot n - 2)$ directions in a $n \times n$ neighborhood [20].

By considering the origin $(0, 0)$ of an image grid of size $M \times N$ as its upper left corner, we can define the coordinates (x, y) of a test point, in a given direction α , as follows:

$$\begin{aligned} x &= x_{center} - k \cdot \sin(\alpha) \\ y &= y_{center} + k \cdot \cos(\alpha), \end{aligned}$$

for all k such that $-\frac{n}{2} \leq k \leq \frac{n}{2}$. x_{center} and y_{center} are the coordinates of the center of the considered $n \times n$ neighborhood.

This procedure is repeated for all D directions $(0..D-1)$ by changing the value of α accordingly ($\alpha = 0, 1 \cdot \frac{180}{D}, 2 \cdot \frac{180}{D}, \dots, (D-1) \cdot \frac{180}{D}$). Figure 3 illustrates test points for $\alpha = 45^\circ$ and $n = 9$.

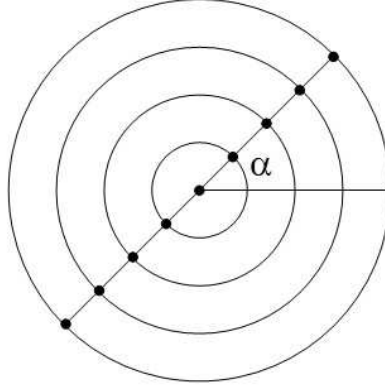


Figure 3: Test points for $\alpha = 45^\circ$ and $n = 9$.

Finally, our orientation field image d can be defined by the following steps:

1. Set D to the number of directions to be considered and n to at least $\frac{D+2}{2}$. Then, consider an information parameter describing the homogeneity degree of the corresponding test points for each of the D directions. An example of such a parameter, used in this work, is the standard deviation σ . In terms of implementation, one can store these data into an array $Sd[i]$, where $i \in \{0, 1, \dots, D-1\}$.
2. The standard deviation value of each considered direction is compared with the one in its perpendicular direction, that is, the value $Sd[i]$ is compared with $Sd[i + \frac{D}{2}]$, $i \in \{0, 1, \dots, \frac{D}{2} - 1\}$ and $i + \frac{D}{2}$ is the corresponding perpendicular direction.
3. The pair of directions i and $i + \frac{D}{2}$ exhibiting the highest information contrast, in a given pixel (e.g., $\max\{|Sd[i] - Sd[i + \frac{D}{2}]|\}$), define the new image d as follows:

$$d(x, y) = \begin{cases} i, & \text{if } Sd[i] < Sd[i + \frac{D}{2}] \\ i + \frac{D}{2}, & \text{if } Sd[i] > Sd[i + \frac{D}{2}] \\ \text{none}, & \text{otherwise} \end{cases}$$

Image d can be seen as a directional image having values in the discrete range $[0, D - 1]$ related to a contrast measure defining the strength of the information parameter (the standard deviation) along a certain direction.

Figure 4 shows an idealized 3D representation of a fingerprint. Intuitively, we can see that the standard deviation value along the ridges or valleys is smaller than the one computed in its perpendicular direction.

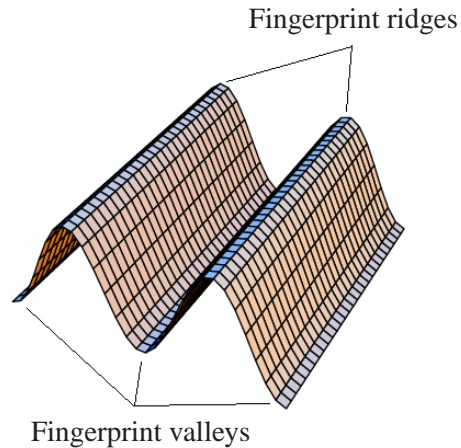


Figure 4: Idealized 3D representation of a fingerprint.

The final result of the algorithm for orientation field estimation, when applied to a fingerprint image (figure 5(a)), is shown in figure 5(b).

3.1.1 Filtering the orientation field image

The algorithm described above defines a directional image whose pixels indicate the orientation of the image components with respect to a neighborhood of size $n \times n$ which is proportional to the number of considered directions D . Due to the discrete domain of the image and its limitations in accurately representing all the directions in a given neighborhood, some pixels may have locally uncorrelated values, thus yielding a noisy version of the directional information.

A common solution to this problem consists in splitting the image into blocks of size $W \times W$ and replacing each pixel of a block by the direction exhibiting the highest frequency inside this block.

This block-wise approach is coarse since it hides image details and causes abrupt direction changes from one block to another. So, in order to obtain a finer orientation field information, we consider a pixel-wise approach in which a block of size $W \times W$ is centered at a given pixel and the direction exhibiting the highest frequency inside the block is attributed to this central pixel. From now on, we refer to the block used in our pixel-wise approach as a *smoothing window* Ω .

The block-wise and the pixel-wise filtering methods are illustrated in figures 5(c) and 5(d), respectively, for the original fingerprint image in figure 5(a).

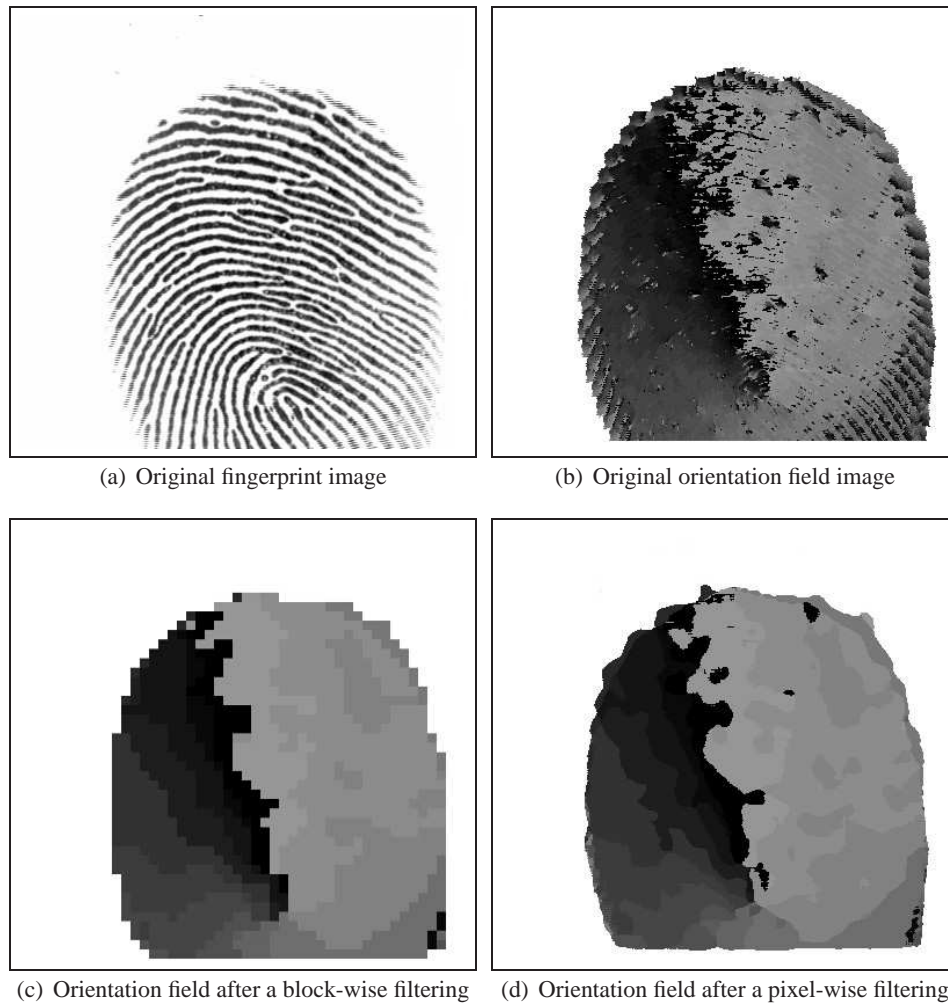


Figure 5: Orientation field estimation for a fingerprint image ($D = 16$, $n = 15$). For the purpose of visualization, each direction in (b,c,d) is represented by a gray-scale value ranging from 0 to 150, in steps of 10, and defined in degrees as $\frac{f(x,y)}{10} \cdot 11.25$.

3.1.2 The orientation field of broken ridges

The algorithm described so far has proved to be very robust even in cases of fingerprint image problems involving noise, acquisition from dry or wet fingers, shadows from late fingerprints, etc. Nevertheless, in cases of components with large regions of broken ridges caused, for instance, by cuts or scars (see figure 6(a)), the detected orientation corresponds to a direction perpendicular to the actual ridge orientation. Thus, the regions associated with the disconnected ridges are represented in the directional image d by an abrupt change of orientation, as shown in figure 6(b). The use of this information, together with the filtering operation by different smoothing windows Ω , will be explored here to detect the pixels between disconnected ridges.

Indeed, as we will see next, the filtering of the directional image by a smoothing window of increasing size defines a multiscale representation of this image conveying useful information about the components connectivity. In a general way (see figure 6 for illustration), we have that a filtering of the directional image, by a small window Ω (figure 6(b)), yields a finer representation of the orientation field than the one obtained with larger windows Ω (figures 6(c) and (d)).

This multiple representation of the directional information can be used to define the regions between disconnected components of an image as follows:

1. Define two images d_s and d_l corresponding to the directional image d filtered with a small (Ω_s) and a large (Ω_l) smoothing window of sizes $(2s + 1) \times (2s + 1)$ and $(2l + 1) \times (2l + 1)$, respectively, where $s, l \in \{1, 2, \dots, \min(\frac{M}{2}, \frac{N}{2})\}$ and $s < l$. Image d_s is a finer smoothed version of the directional information, while d_l is a coarser version. Note that d corresponds to the finest representation of the directional image smoothed by a window Ω_s with $s = 0$.
2. Rectify the finer representation of the directional image d , d_s , by taking into account the pixel-wise perpendicularity between images d_l and d_s as follows:

$$d'_s(x, y) = \begin{cases} d_l(x, y), & \text{if } d_l(x, y) \perp d_s(x, y) \\ d_s(x, y), & \text{otherwise} \end{cases}$$

3. Consider a set X as the pixels of d_s updated by the above operation, that is,

$$(x, y) \in X, \text{ if } d_s \neq d'_s, \forall (x, y) \in \mathcal{D}_{d_s}$$

This set corresponds to the regions between broken ridges and will be used further in the reconnection procedure.

Note that this operation corrects the finer directional information along the disconnected components of the original image by changing the value of the pixels not filtered at a finer scale and represented by a local change of orientation along the image components.

Figure 6 illustrates the above steps for a fingerprint image with some broken ridges. Figure 6(b) shows the original orientation field of the image in figure 6(a) after a filtering process with a smoothing window Ω_s of size 15×15 . A coarser scale of this information, defined by a filtering with a 45×45 smoothing window Ω_l , is shown in figure 6(d). Figure 6(e) corresponds to the orientation field in figure 6(b) rectified according to step 2 above. The difference between the rectified orientation field (figure 6(e)) and its original finer version (figure 6(b)) determines the set X shown in figure 6(f) which represents the regions between the broken ridges.

3.2 Image enhancement by watersheds

As stated in section 2.3, the watershed algorithm constitutes a powerful morphological tool used for segmenting regions based on the set of image minima.

In a general way, the final result of the watershed transform applied to fingerprints should have the following characteristics:

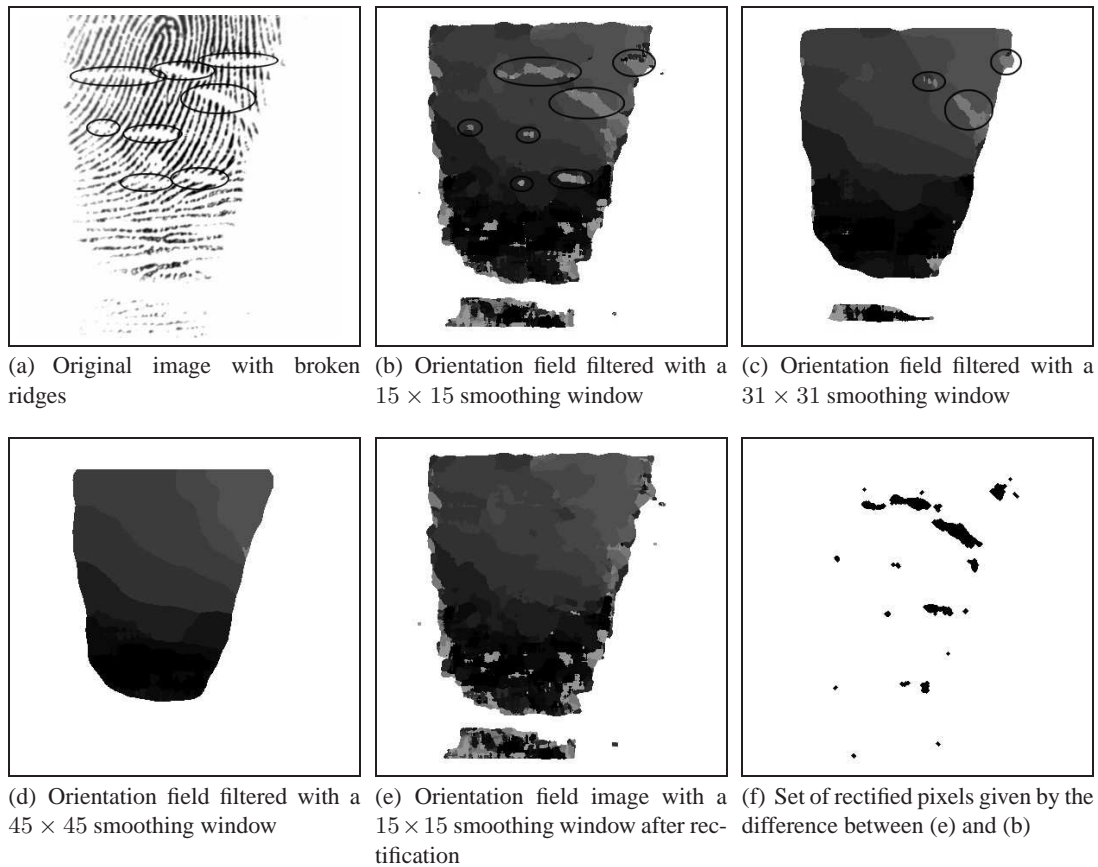


Figure 6: Examples of different scales (b, c, d) of a directional image and the orientation field rectification (e) based on a coarser directional image. The highlighted areas show the broken ridges and the directions improperly defined with respect to this coarser directional information (a directional image filtered by a large smoothing window).

- Ideally, each fingerprint ridge, considered here as the valleys of the original image, should define a basin surrounded by the corresponding watershed lines. Naturally, this is the case for binary images since for gray-scale ones a single ridge can have more than one minimum which, after the watershed transformation, relates one ridge to a set of k basins, $k \geq 1$.
- Ideally, the watershed lines should be exclusively defined in the regions between ridges (the regional maxima) or, in cases of disconnectedness, in the regions between broken ridges. However, since each ridge in the gray-scale case can have more than one regional minimum, the corresponding watershed lines may also cross the ridges perpendicularly with respect to their dominant direction.

Figure 7(b) illustrates a fingerprint image segmentation by watersheds. In order to reconnect the broken ridges, we define a set of markers based on the original image watershed lines, as explained next.

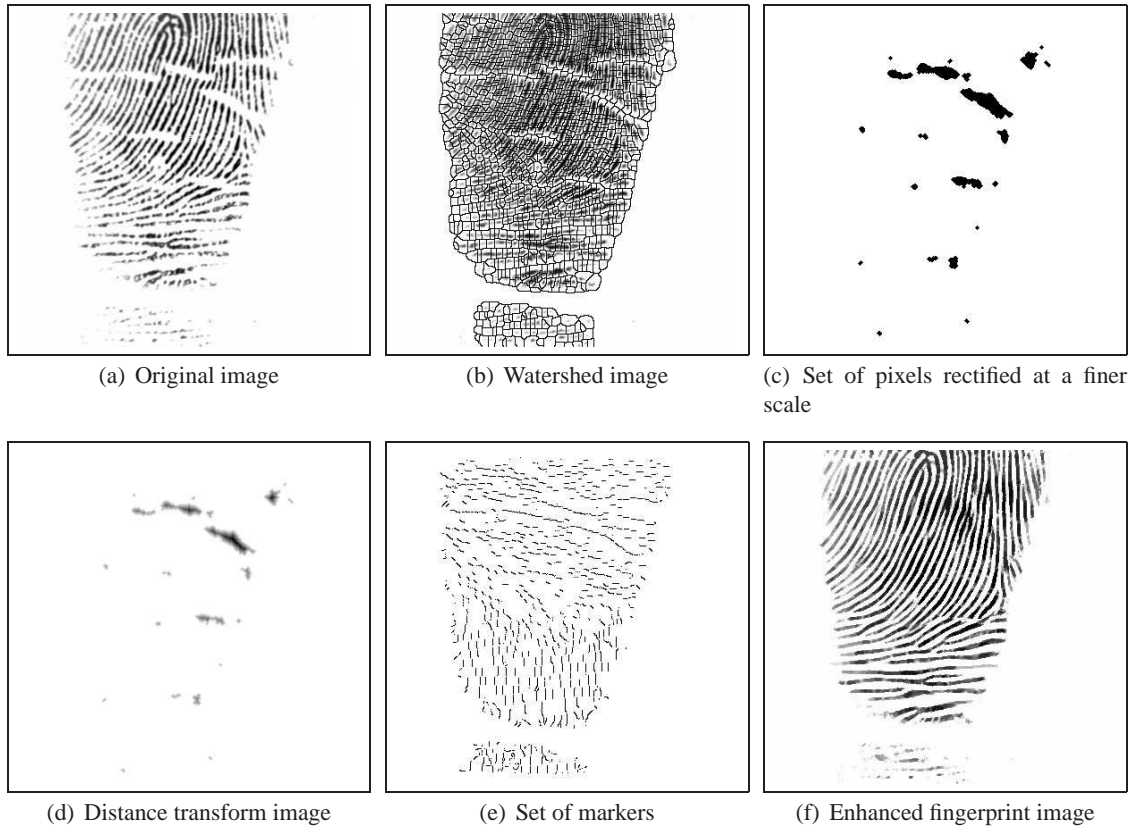


Figure 7: Example of the operations used to reconnect the broken ridges of a fingerprint image.

3.3 Definition of markers

Given the set of watershed lines of a fingerprint image, no matter if it is in the ideal segmentation case or not, we can combine this topographic information with the orientation field image (section 3.1.2) to define a subset of the watershed lines to be used as markers of the regions between broken ridges.

Let M be this subset and $L = \{l_1, l_2, \dots, l_n\}$ the set of the original watershed lines. Informally, each line l_i is defined as the set of pixels between two bifurcations of the watershed lines (pixels whose connectivity number equals 2 for an 8-connected neighborhood [22]).

Now, consider the orientation field estimation (section 3.1) of the watershed image. Note that, in such a case, we apply the algorithm described in section 3.1 on a binary image. If the orientation of a line l_i of the set L is perpendicular to the ridge direction (a pixel-wise comparison between the orientation fields of the watershed and the original images provides this information), then it is very likely that l_i belongs to a region between broken ridges or between regional minima of these ridges (see figure 7(b)). In such a case, l_i should be added to the set of markers M . Otherwise, if l_i has the same ridge direction, then it is just defining the boundary between adjacent ridges and, therefore, should not be taken into account here.

The definition of the subset of the watersheds, representing markers for the regions between broken ridges, can be summarized by the following pseudocode:

```

M = ∅
For all line  $l_i \in L$  do
  If  $l_i$  is perpendicular to the ridge direction do
     $M \leftarrow M \cup l_i$  /* Update the markers set */

```

3.4 Estimation of the distance between broken ridges

The next step of our approach consists in estimating the distance between broken ridges in order to reconnect them properly.

For this purpose, we apply the distance transform [23] to the set X defined from the difference between the orientation field images at two different scales, as explained in section 3.1.2. This set corresponds to pixels between broken ridges whose directional value was improperly defined at a finer scale (orientation field image filtered by a small smoothing window Ω_s).

Figure 7(d) shows the distance transform applied to the image in figure 7(c) representing the set of rectified pixels of the image in figure 6(b). Finally, the distance between the closest broken ridge to a given point of l_i , belonging to set X , can be defined as $(2 \cdot dt + 1)$, where dt is the distance transform value at this point.

3.5 Directional opening by markers

The set M defined in section 3.3 marks the regions considered in our last step which reconnects ridges and enhances the whole fingerprint image. This procedure can be accomplished by a morphological directional opening taking into account the markers l_i in set M , the distance transform of the components in set X , and the information at a certain scale of the orientation field image.

Shortly, the reconnection of the broken ridges can be obtained by implementing, for each point of a marker l_i belonging to the set X , a morphological opening on a line segment of length $(2 \cdot dt + 1)$ by a linear structuring element of the same size, centered at this point. The orientation of this opening corresponds to the ridge direction given by the orientation field image.

The same directional opening is defined for those markers l_i , belonging to regions between broken ridges, whose directional information was properly defined at a finer scale. Note that these regions are not included in set X and, in such a case, the length of the considered linear structuring element should be small (e.g., 5) and proportional to the size of the window Ω_s .

Figure 7 illustrates the main steps of our reconnection procedure for the original image in Figure 7(a), and Figures 8(e)-(h) show the final results of the method applied to several fingerprint images in Figures 8(a)-(d). All these results were obtained by considering the following parameters: $D = 16$ directions, $n = 9$ test points and smoothing windows Ω_s and Ω_l of sizes 15×15 and 45×45 , respectively.

The fingerprint images used as examples were obtained from the FVC2002 (Fingerprint Verification Competition) databases [24].

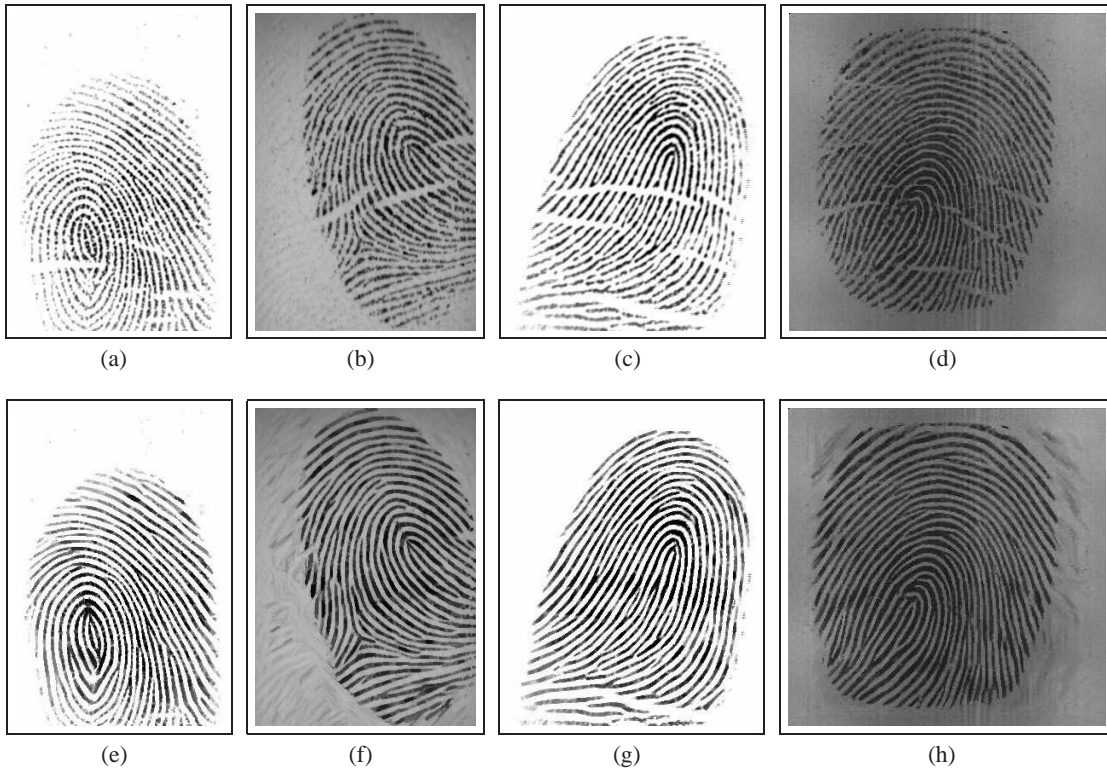


Figure 8: Other examples of our approach with $D = 16$ directions, $n = 9$ test points and smoothing windows Ω_s and Ω_l of sizes 15×15 and 45×45 , respectively. (a,b,c,d) Original fingerprint images. (e,f,g,h) Enhanced images.

4 Conclusions

This work introduced a multiscale operator that extracts directional information from image components. This operator has proved to outperform the existing approaches in its pixel-wise accuracy and can be used in binary and gray-scale images.

We also developed a morphological approach for reconnecting broken ridges of fingerprint images which can be easily extended to connect image components whose features can be described by directional information. This problem concerns many image processing applications, for example, in medicine, biometrics, metallurgy and geology.

As future works, we intend to apply the proposed multiscale operator in new problems including image segmentation and classification.

Acknowledgements

The authors are grateful to FAPESP for supporting this work through the project number 03/01907-8.

References

- [1] D. Maltoni, D. Maio, A. K. Jain, and S. Prabhakar. *Handbook of Fingerprint Recognition*. Springer, New York, 1st edition, 2003.
- [2] A. K. Jain, S. Prabhakar, and S. Pankanti. On the similarity of identical twin fingerprints. *Pattern Recognition*, 35:2653–2663, 2002.
- [3] A. Jain, L. Hong, and R. Bolle. On-line fingerprint verification. *IEEE Transactions on Pattern Analysis and Machine Intelligence*, 19(4):302–313, April 1997.
- [4] D. Maio and D. Maltoni. Direct grays-scale minutiae detection in fingerprints. *IEEE Transactions on Pattern Analysis and Machine Intelligence*, 19(1):27–39, January 1997.
- [5] L. Hong, Y. Wan, and A. Jain. Fingerprint image enhancement: Algorithm and performance evaluation. *IEEE Transactions on Pattern Analysis and Machine Intelligence*, 20(8):777–789, August 1998.
- [6] Y. He, J. Tang, X. Luo, and T. Zhang. Image enhancement and minutiae matching in fingerprint verification. *Pattern Recognition Letters*, 24, 2003.
- [7] B. G. Sherlock, D. M. Monro, and K. Millard. Fingerprint enhancement by directional fourier filtering. *IEEE Proceedings in Visual Image Signal Processing*, 141(2):87–94, April 1994.
- [8] A. J. Willis and L. Myers. A cost-effective fingerprint recognition system for use with low-quality prints and damaged fingertips. *Pattern Recognition*, 34:255–270, 2001.
- [9] C. Hsieh, E. Lai, and Y. Wang. An effective algorithm for fingerprint image enhancement based on wavelet transform. *Pattern Recognition*, Volume 36:303–312, 2003.
- [10] S. Greenberg, M. Aladjem, and D. Kogan. Fingerprint image enhancement using filtering techniques. *Real Time Imaging*, 8:227–236, 2002.
- [11] J. Yang, L. Liu, T. Jiang, and Y. Fan. A modified gabor filter design method for fingerprint image enhancement. *Pattern Recognition Letters*, 24:1805–1817, 2003.
- [12] Q. Xiao and H. Raafat. Combining statistical and structural information for fingerprint image processing classification and identification. *Pattern Recognition: Architectures, Algorithms and Applications*, pages 335–354, World Scientific, River Edge, NJ, 1991.
- [13] D.C.D. Hung. Enhancement and feature purification of fingerprint images. *Pattern Recognition*, 26(11):1661–1671, 1993.
- [14] A. Farina, Z.M. Kovacs-Vajna, and A. Leone. Fingerprint minutiae extraction from skeletonized binary images. *Pattern Recognition*, 32(5):877–889, 1999.
- [15] B. Bhanu, M. Boshra, and X. Tan. Logical templates for feature extraction in fingerprint images. *Proc. Int. Conf. on Pattern Recognition (15th)*, 2:850–854, 2000.

- [16] D. Maio and D. Maltoni. Neural network based minutia filtering in fingerprints. *Proc. World Conf. on Systems Cybernetics and Informatics*, 4:1654–1658, 1998.
- [17] J. Chang and K. Fan. A new model for fingerprint classification by ridge distribution sequences. *Pattern Recognition*, 35:1209–1223, 2002.
- [18] J. Serra. *Image Analysis and Mathematical Morphology*. London, Academic Press, 1982.
- [19] J. Serra. *Image Analysis and Mathematical Morphology - Volume 2 : Theoretical Advances*. 1988.
- [20] P. Soille. *Morphological Image Analysis. Principles and Applications*. Springer Verlag, 1999.
- [21] S. Beucher and S. F. Meyer. *The morphological approach to segmentation: The Watershed Transformation*. E. Dougherty (ed). Marcel Decker Inc., New York, 1992.
- [22] S. Yokoi et alli. An analysis of topological features at digitized binary pictures using local features. *Computer Graphics and Image Processing*, 4:63–73, 1975.
- [23] A. Rosenfeld and A.C. Kak. *Digital Picture Processing*, volume I and II. Academic Press, Orlando, Florida, 1982.
- [24] FVC2002 Fingerprint Verification Competition. <http://bias.csr.unibo.it/fvc2002/>.